The high-pressure structural sequence of phosphorus is strikingly different to that of its heavier congeners....

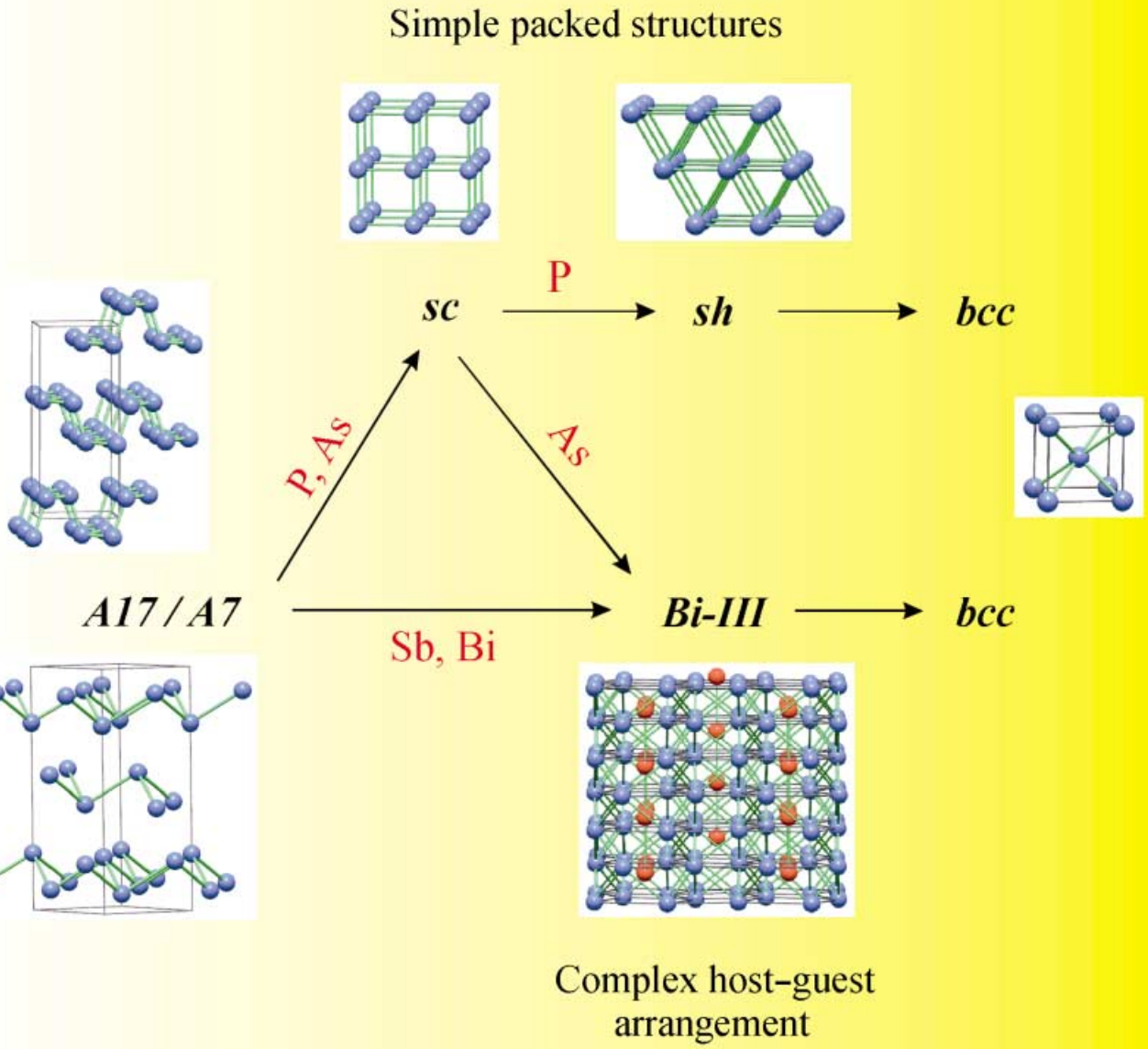

...DFT calculations reveal, that s-d band mixing under pressure plays a key role for an understanding of the stability of Group 15 element high-pressure structures. For more information read on . . .

  0947-6539/03/0907-1471 $ 20.00+.50/0

High-Pressure Structural Trends of Group 15 Elements: Simple Packed Structures versus Complex Host–Guest Arrangements

Ulrich Häussermann*[a]

Abstract: The Group 15 elements P, As, Sb, and Bi all have layered structures consisting of six-membered rings under ambient conditions and attain the body-centered cubic (bcc) structure at the highest pressures applied. In the intermediate pressure region, however, phosphorus and its heavier congeners behave profoundly differently. In this region P first attains the open packed simple cubic (sc) structure for a wide range of pressures and then transforms into the rarely observed simple hexagonal (sh) structure. For the heavier congeners complex, incommensurately modulated host–guest structures emerge as intermediate pressure structures. We investigated the high-pressure behavior of P and As by ab initio density functional calculations in which pseudopotentials and a plane wave basis set were employed. The incommensurately modulated high-pressure structure of As was approximated by a supercell. Our calculations reproduced the experimentally established pressure stability ranges of the sc and sh structures for P and the host–guest structure for As very well. We found that the sc and especially the sh structure are decisively stabilized by the admixture of d states in the occupied levels of the electronic structure. This admixture releases s–s antibonding states above the Fermi level (s–d mixing). With pressure, s–d mixing increases rapidly for P, whereas it remains at a low level for As. As a consequence, the band energy contribution to the total energy determines the structural stability for P in the intermediate pressure region, giving rise to simple packed structures. On the other hand, in the intermediate pressure region of the heavier Group 15 elements, a delicate interplay between the electrostatic Madelung energy and the band energy leads to the formation of complex structures.

Keywords: ab initio calculations · bond theory · high-pressure chemistry · pnicogens · polymorphism

Introduction

High-pressure experiments, which allow the study of the structural stability as a function of volume, have added a new dimension to the fundamental question concerning the relation between atom arrangement and electronic structure. Of particular importance is the understanding of elemental structures, and in this respect recent high-pressure investigations of main-group elements have yielded many surprising and intriguing results. For example, it was found that at high pressures the simple metal Li undergoes a transition to a low-coordinate structure and becomes semimetallic.[1] Rb and Cs attain a remarkable complexity in the high-pressure structures of Rb-III[2] and Cs-III,[3] which contain 52 and 84 atoms in the unit cell, respectively. An even more complex structure has recently been found for Ga (Ga-II).[4] Interestingly, the structures of Rb-III, Cs-III, and Ga-II are closely related when they are considered as stackings of different layers. Finally, Sr,[5] Ba,[6] and the heavier Group 15 elements As, Sb, and Bi[7a] adopt structures with two interpenetrating components, a host and a guest structure, which are incommensurate with each other.[7b]

The occurrence of a host–guest structure in an element, where the host and guest is formed by the same component, is most unusual and has attracted much attention.[8] Recently, we performed a calculational study of the high-pressure behavior of the heavier Group 15 elements As, Sb, and Bi.[9] We found a supercell approximation for the incommensurate host–guest structure which reproduced the experimentally established pressure stability ranges extremely well. Herein the focus is on the striking difference between the high-pressure behavior of P and that of its heavier congeners. Importantly, under pressure P does not display a complex host–guest structure. Instead, the high-pressure structural sequence of this element is dominated by the simple cubic (sc) and simple hexagonal (sh) structure which otherwise are rarely observed as elemental structures. The high-pressure behavior of P and As was investigated by ab initio calculations employing pseudopotentials and a plane wave basis set. Arsenic is taken as a representative for the heavier Group 15 elements. With this study we aim to rationalize the high-

[a] Dr. U. Häussermann
Department of Inorganic Chemistry
Stockholm University, 10691 Stockholm (Sweden)
E-mail: ulrich@inorg.su.se

  0947-6539/03/0907-1472 $ 20.00+.50/0

pressure structural sequences of Group 15 elements and establish general electronic structure trends for a wide range of compression, which covers all experimentally reported phase transitions. In particular, we try to find the reasons behind the stability of simple packed structures in phosphorus and the existence of complex structures at intermediate pressures in As, Sb, and Bi.

Results and Discussion

High-pressure structural transitions of Group 15 elements

Summary of experimental findings: The experimentally establised high pressure behavior (at room temperature) of the Group 15 elements P, As, Sb, and Bi is summarized in Figure 1. At ambient pressure phosphorus possesses the orthorhombic A17 structure (Figure 2a), whereas the heavier Group 15 elements adopt the rhombohedral A7 structure (Figure 2b).[10] Both structures can be described as consisting of layers of six-membered rings in the chair conformation, which are connected differently in the two structures. Each atom has three short contacts in the layer and three longer contacts with the atoms of one adjacent layer. The layered character appears more pronounced in the A17 structure. It is well known that the A17 and A7 structures are related to the simple cubic structure.[11] This is especially apparent for the A7 structure, for which the atoms attain a distorted octahedral (3 + 3) coordination (Figure 2c).

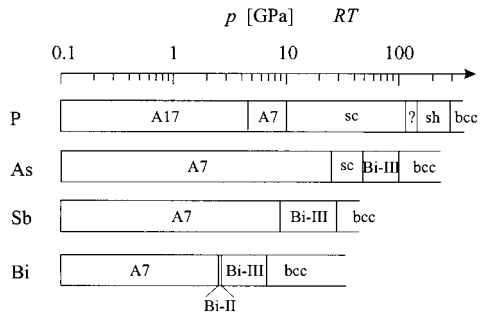

Figure 1. High-pressure structural behavior of P, As, Sb, and Bi established by experiment (at room temperature).

As the pressure is increased, P transforms first at about 5 GPa from the A17 ground state structure to the A7 structure[12, 13] and then at about 10 GPa into the sc structure.[12, 13] As transforms at 25 GPa from the A7 ground state structure to the sc structure (As-II).[14] For Sb the sc structure is closely approached,[15] but the first structural high-pressure transition at 8.6 GPa results in tetragonal Sb-II with the Bi-III structure.[16] Bi transforms already at 2.77 GPa via the Bi-II structure into Bi-III.[17] The structure of Bi-III (Figure 2d) has long-been uncertain and was only recently identified as a complex incommensurate host–guest structure.[7] The host consists of 3^2434 nets that are stacked in antiposition. This yields a tetragonal assembly of rows of square antiprisms in which linear chains of guest atoms are located. The guest structure corresponds to a body-centered tetragonal (bct) array that is incommensurate with the host along the *c* direction. At 137 GPa P transforms from the sc structure via an intermediate structure to the sh structure (Figure 2e).[18] In contrast, As transforms already at about 48 GPa from the sc structure into a slightly modified Bi-III structure with a monoclinic guest arrangement.[7a, 19] At the highest pressure applied the Group 15 elements adopt the body-centered cubic (bcc) structure (Figure 2f). The bcc structure represents the current end-member of the high-pressure structural series of P, As, Sb, and Bi and is obtained at pressures of 262,[20] 93,[19] 28,[21] and 7.7 GPa,[22] respectively.

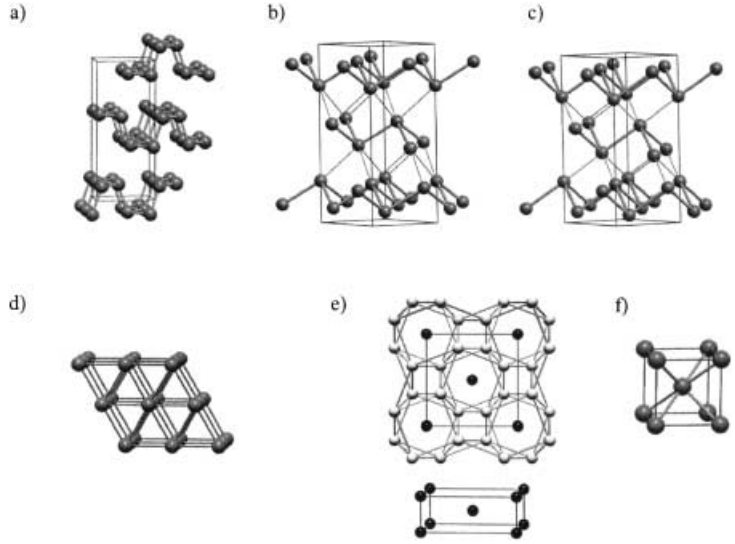

Figure 2. a) The orthorhombic A17 ground state structure of P shown approximately along [100]. b) The rhombohedral A7 ground state structure of As, Sb, and Bi shown approximately along [1$\bar{1}$0]. Thicker gray lines denote short intralayer atomic distances, thin gray lines the long interlayer ones. In the simple cubic (sc) structure of P-III and As-II (c) interlayer and intralayer distances have equal length. d) The simple hexagonal (sh) structure of P-V. e) The tetragonal Bi-III structure shown along [001]. Host atoms: light gray, guest atoms: black. The guest structure, which is additionally depicted separately below, is incommensurate with the host along [001]. f) The bcc structure as adopted by P-VI, As-IV, Sb-III and Bi-V.

We summarize the high-pressure structural sequences of the Group 15 elements in Scheme 1. P behaves profoundly differently from its higher congeners in the intermediate pressure region. For P this region is dominated by the simple packed structures sc and sh, which have large stability ranges of at least 100 GPa. In contrast As, Sb, and Bi prefer complex host–guest arrangements. Before transforming into the host–guest structure, As also adopts the sc structure. However, the sc-As phase is stable in a rather limited pressure range. Further, untypical for the heavier element, the transition A7 → sc occurs at higher compressions than for P. The simple packed structures

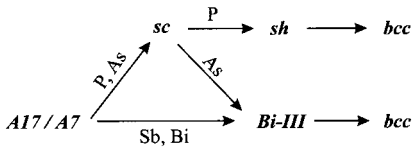

Scheme 1. Summary of the high-pressure structural sequences of the Group 15 elements.

sc and sh are rare in the Periodic Table. Apart from P and As, the sc structure occurs in ground state Po[10] and in a high-pressure modification of Ca.[23] The sh structure is only known in high-pressure phases of P,[13] Si,[24] and Ge.[25] Interestingly, the simple packings realized in P exhibit by far the highest pressure stability: The high-pressure stability ranges of the other elemental simple packings do not exceed 25 GPa.

Calculational results: Figure 3 summarizes our results concerning the high-pressure behavior of P and As. It displays calculated enthalpy differences $H - H_{A7}$ (relative to the A7 structure) for the elements in the considered structures as a function of pressure. For P we find the sequence of transitions A17 → 2.4 GPa → A7 → 12.3 GPa → sc → 135 GPa → sh → 293 GPa → bcc, which is in satisfactory agreement with the experimental findings. Individual high-pressure transitions have been the subject of earlier theoretical investigations. In 1986 Chang and Cohen examined the A17 → A7 and A7 → sc transitions.[26] They obtained 3 GPa for the first transition, but could not find the second transition from their calculations. Some years later the A7 → sc transition was then properly described in the works by Sasaki et al., who determined the transition pressure to be 15.8 GPa.[27, 28] The sc → sh transition was examined recently by Nishikawa et al.[29] These authors estimated the transition pressure to be 121 GPa, which is in good agreement with our result.

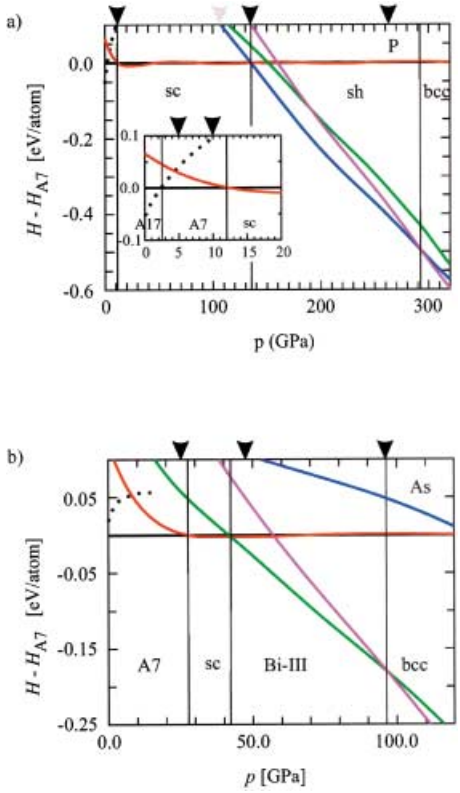

Figure 3. Calculated enthalpy differences (relative to the A7 structure) for P (a) and As (b) as a function of pressure. Black, dotted: A17 structure, black: A7 structure, red: sc structure, green: Bi-III structure, blue: sh structure, magenta: bcc structure. The pressure stability ranges of the considered structures are indicated by vertical lines (calculated, zero temperature) and black markers (experimental, room temperature). The gray marker in a) indicates the experimental transition from sc-P to intermediate P-IV with unknown structure. The inset in a) represents a close up of the low-pressure region where the first structural transitions occur.

From the enthalpy differences in Figure 3a it becomes especially apparent that in P the host–guest Bi-III structure never becomes competitive with the simple packed sh structure. The latter is almost constantly by 0.05 eV per atom lower in enthalpy over the whole pressure range of its existence. The flexible *c*/*a* ratio of the sh structure varies only slightly with pressure. According to the experimental results there is an increase from 0.948 to 0.956 when pressure is increased from 137 to 280 GPa.[20] Our calculations show an increase of the *c*/*a* ratio from 0.946 to 0.953 within this pressure range, which is in very good agreement with the experimental values (Figure 4). Thus, in the sh structure of P the interatomic distances along the axial direction are about 5% shorter than the ones in the hexagonal plane, and the coordination number can be described as 2 + 6.

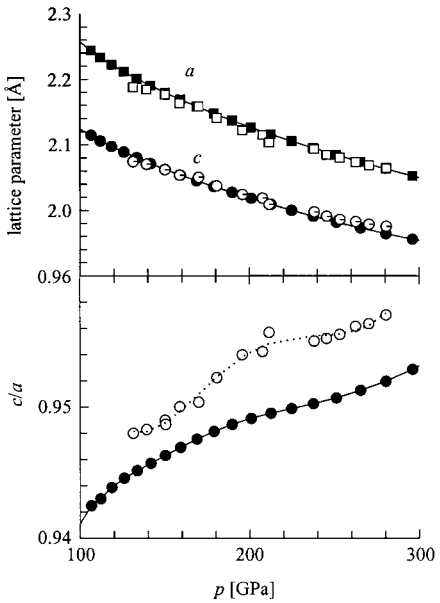

Figure 4. Pressure dependence of the lattice constants of the sh-P phase and its *c*/*a* ratio. Open symbols indicate the experimental data according to reference [20], filled symbols correspond to calculated results.

Turning to As, we find the following phase transition sequence with increasing pressure: A7 → 28 GPa → sc → 43 GPa → Bi-III → 97 GPa → bcc (Figure 3b). This compares extremely well with the experimental (room-temperature) transition pressures. The first structural transition As → sc has been the subject of earlier theoretical investigations.[30, 31, 32] The transition pressures predicted in these works ranged between 20 and 35 GPa. Interestingly, for As the sh structure

0947-6539/03/0907-1474 $ 20.00+.50/0 *Chem. Eur. J.* **2003**, *9*, No. 7

represents the most unfavorable alternative among the considered structures at intermediate and high pressures. Concerning the structure of As-III we applied two approximations: First, we described As-III by the Bi-III type structure with a bct arrangement of the guest structure and did not take into account the possibility of a monoclinic distortion.[7] Second, the incommensurate host–guest structure was approximated by a supercell because conventional electronic structure calculations are based on periodic boundary conditions. A detailed description of the Bi-III type model structure can be found in reference [9].

In conclusion, our calculations could reproduce the high-pressure behavior of P and As in a highly satisfacory manner. In the next step we analyze the electronic structure trends for P and As under pressure. This should reveal the origin of the different high-pressure behavior within the Group 15 elements.

Electronic structure changes under pressure

Density of states: We computed the electronic density of states (DOS) of P and As in the ground state and high-pressure structures and assembled the obtained curves in Figure 5. Figure 5a compares the electronic structures of P in the A17 with that of As in the A7 structure at the respective ground state volumes. Most conspicuous is the characteristic splitting of the DOS into four parts: s–s bonding, s–s antibonding, p–p bonding, and p–p antibonding. Owing to the atomic electron configuration of P and As the Fermi level is situated between the p–p bonding and antibonding bands. The Fermi level is at a narrow band gap in A17-P and in a deep pseudo gap with a very low value of density of states in A7-As. This is in agreement with the electronic properties of these materials.

With increasing pressure, P transforms from the A17 to the A7 structure. The DOS of A7-P is virtually identical to the DOS of A7-As at a volume close to the transition to sc-As (Figure 5b). Both elements remain pronounced semimetals. Figure 5c displays the DOS of sc-P and sc-As at volumes slightly above the respective transition pressures. Again, the DOS curves of both elements are very similar. Compared to the A7 structure, the density of states at the Fermi level is drastically increased in the sc structure, and the deep pseudo gap separating p–p bonding from antibonding states has changed into a shallow, although marked, well.

Figure 5d shows the DOS of Bi-III type As-III and sh-P at a volume approximately corresponding to the center of the respective pressure stability ranges. Now, the differences in the high-pressure behavior of P and As become also apparent in their electronic structures. For Bi-III type As, the overall shape of the DOS curve is reminiscent of that of sc-As, apart from the spikey feature which is due to the complexity of the Bi-III structure. As in A7-As and sc-As the s and p bands are energetically separated, that is their overlap is rather limited. Further, the Fermi level of Bi-III type As is still located at a recognizable valley in the p bands. This persistence of the p band bonding–antibonding splitting indicates a still significant covalent p–p bonding in the host–guest structure. Thus, the structural transition sc → Bi-III in As is accompanied with a smooth variation in the electronic structure. This is completely different for P: In sc-P at higher compressions (not shown) and sh-P s and p bands overlap heavily and the p band bonding–antibonding splitting has disappeared. At the same time the d state contribution to the occupied bands has increased considerably. The DOS of P and As in the bcc structure at a volume slightly above the respective transition pressures are displayed in Figure 5e. We observe that for bcc-As the Fermi level is no longer situated in a well and that the DOS curves of bcc-P and bcc-As attain an approximately parabolical nearly-free-electron distribution. However, in bcc-As s and p bands are still separated to a large extent and the admixture of d states in the occupied bands remains at a low level. Thus, as the pressure increases the orbital character of the occupied bands seems to evolve differently for P and As.

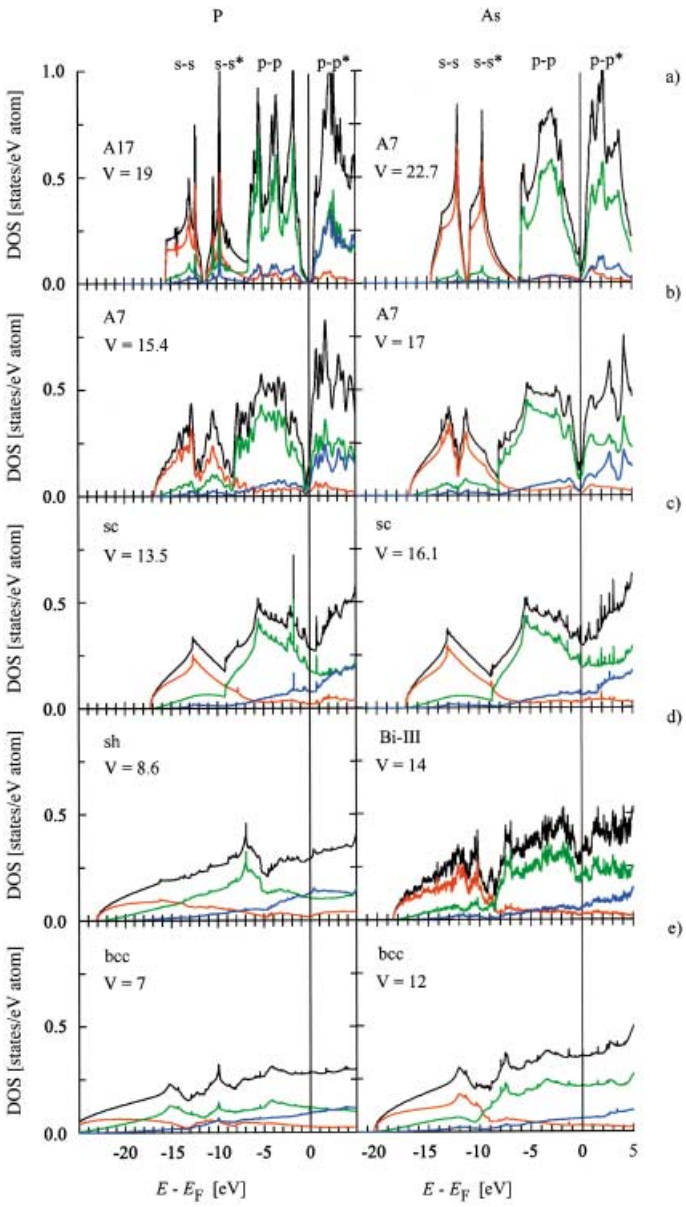

Figure 5. Density of states (DOS) of P and As in the ground state and high-pressure structures. Black: total DOS, red: s-projected DOS, green: p-projected DOS, blue: d-projected DOS.

  0947-6539/03/0907-1475 $ 20.00+.50/0

Structural stability: To understand high-pressure structural transitions it is advantageous to divide the total energy into the band energy E^{band}, which represents the sum over the occupied one-electron states (as presented in Figure 5), and a part containing the remaining contributions, of which the electrostatic (Madelung) energy that includes the repulsion of the positively charged ions, is the most significant. E^{band} favors the formation of open-packed structures in which the atoms are closer to each other and thus covalent bonding can be realized. The electrostatic contributions (summarized as E^{Mad}) display an antagonistic behavior with the tendency to stabilize high-symmetry densely packed structures. In this respect the bcc structure is the most favorable structure of all dense packings (bcc, fcc, hcp), since it has the highest Madelung constant.[33] Clearly, for the Group 15 elements the band energy E^{band} determines the structural stability of the layered A17 and A7 ground state structures. Usually, the E^{Mad} contribution increases relative to E^{band} under compression, and densely packed structures are obtained as high-pressure modifications.

How does the band energy E^{band} for P and As evolve with pressure? To answer this question we analyze the trend in the number of occupied s, p, and d states (N_l). In particular, we calculated the ratios $X_l = N_l/N_{tot}$ (N_{tot} being the total number of occupied states) for P and As in the different structures at different volumes (Figure 6). Generally, in any atom arrangement of Group 15 elements with an electron configuration s^2p^3 the resulting electronic structure will possess a large number of occupied s–s antibonding states. Thus, for these elements optimizing the band energy is equivalent to diminishing the number of s–s antibonding states below the Fermi level, while keeping favorable p–p bonding. Or to put it simply, the band energy will be lowest for the structure that expresses the lowest value of X_s. For the ground state volume and at moderate compressions layered A17 and A7 display the lowest values of X_s among all considered structures for the two elements. It was recently shown by Seo and Hoffmann that this is a result of s–p mixing: Lone pair formation at each site is equivalent to a situation in the band structure where strongly s–s antibonding states are partly raised above the Fermi level, and in exchange, p–p nonbonding or weakly antibonding states are lowered below the Fermi level.[34] This is also seen clearly in the DOS of A17-P, A7-P, and A7-As as presented in Figure 5a and 5b. At higher compressions the admixture of empty d states becomes important, and this stabilizes the simple packed structures. The sc structure attains the lowest values of X_s for P and As at lower volumes. For P at highest compressions the sc structure is succeeded by the sh structure.

The evolution of s–d mixing is nicely seen in the trends displayed by the X_s and X_d curves. X_s and X_d vary in a correlated way with pressure, the former decreasing and the latter increasing. X_p remains more or less constant, apart from the region of highest compression in P. Importantly, for As—and the heavier Group 15 elements in general[9]—s–d mixing increases smoothly with pressure and remains at a rather low level. For P s–d mixing increases rapidly and the X_d values approach 25% at the highest compressions. The increased d state contribution in the occupied levels of sc-P and sh-P was already noted by Sasaki et al.[28] and Nishikawa et al.[29] in their investigations of the A7 → sc and sc → sh transitions, respectively. However, in these works the clear relation between X_s and X_d, that is s–d mixing, was not recognized. Figure 6 also shows clearly that the stabilizing mechanism of s–p mixing especially affects the layered structures and that the one of s–d mixing affects the simple packed structures (sc or sh). Interestingly, for P the trend in the lowest X_s values follows the trend in the structural transitions. The Bi-III type host–guest structure takes an intermediate position between open-packed A17 or A7 and

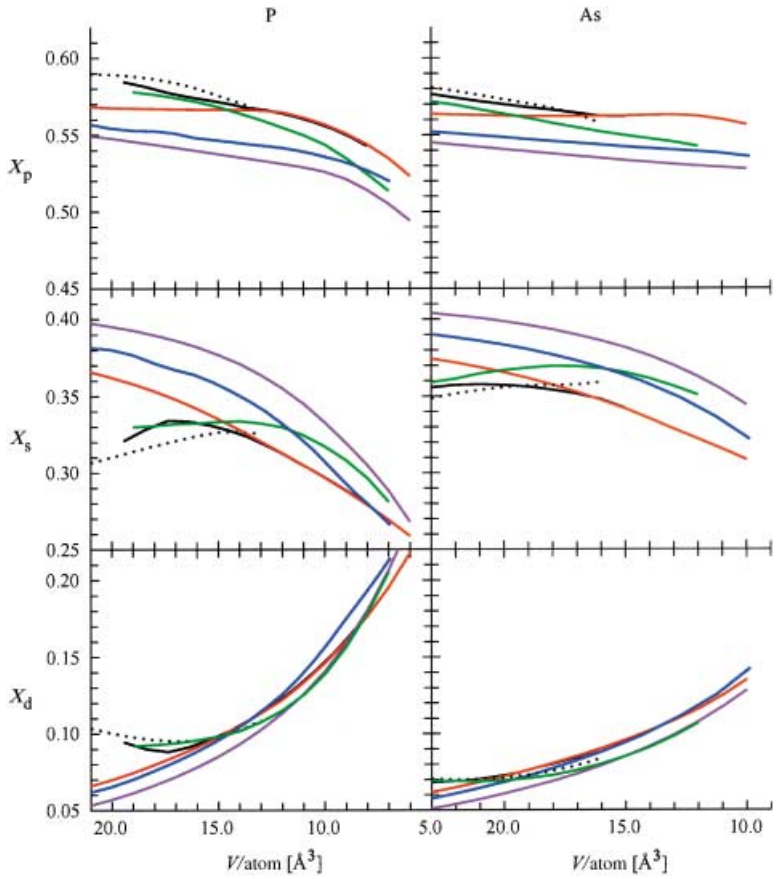

Figure 6. The ratios $X_l = (N_l/N_{tot})$ for P (a) and As (b) as a function of volume. N_l (l = s, p, d) is the number of occupied s, p, and d states, N_{tot} is the total number of occupied states. Black-dotted: A17 structure, black: A7 structure, red: sc structure, green: Bi-III structure, blue: sh structure, magenta: bcc structure.

0947-6539/03/0907-1476 $ 20.00+.50/0 *Chem. Eur. J.* **2003**, *9*, No. 7

densely packed bcc. At low compressions this structure realizes X_1 values close to that of the layered structures and approaches values close to that of the bcc structure with increasing pressure.

In conclusion, structural stability in P follows to a large extent a principle of minimal X_s values, which is achieved by s–p and s–d mixing in the low and intermediate pressure region, respectively. This means that the band energy E^{band} also determines structural stability in the intermediate pressure region and accounts for the stability of the simple packed structures. Thus, the structural changes in P up to pressures of 250 GPa are electronically driven. For As and the heavier Group 15 elements E^{band} governs structural stability only for the ground state and at moderate compressions. In the intermediate pressure range the significance of E^{band} to structural stability lowers and that of E^{Mad} increases. This is illustrated in Figure 7 where we compare ratios E^{Mad}/E^{Mad}_{bcc} as a

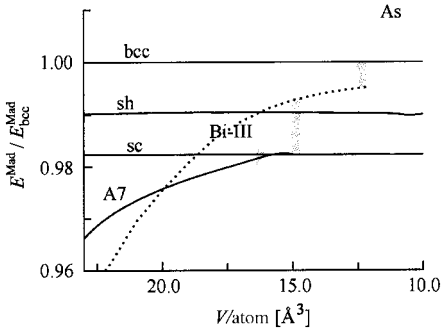

Figure 7. Variation of the electrostatic energies of A7-As, Bi-III-As, sc-As, and sh-As relative to bcc-As as a function of volume. Volume ranges of structural transitions are indicated by gray bars.

function of pressure. The bcc structure with a Madelung constant of 1.79188 is the most favorable arrangement from an electrostatic point of view. The Madelung constants for sc and sh are 1.76012 and 1.77464, respectively. The large structural flexibility of the Bi-III structure implies a flexible E^{Mad} with pressure. At low compression the Bi-III structure attains an electrostatic energy that is similar to that of the layered structures and at high compressions a situation close to that of the bcc structure is approached. In the volume range of the structural transition sc → Bi-III in As the electrostatic energy of the Bi-III structure is more favorable than that of the sh structure. At the same time the X_s values corresponding to this volume range are very similar for Bi-III and sh (cf Figure 6), which means that the E^{band} contribution to the total energy should be comparable in both structures. Thus, the formation of the Bi-III type host–guest structure can be thought of as a consequence of a delicate interplay of E^{band} and E^{Mad} in the intermediate pressure regions of the heavier Group 15 elements, that is both important parts of the total energy account equally for structural stability. Finally, at high pressures E^{Mad} governs structural stability for all Group 15 elements and the densely packed bcc structure is formed for electrostatic reasons.

The high-pressure behavior of the Group 15 elements P, As, Sb, and Bi can be rationalized by their different ability to s–p and s–d mixing. The degree of s–p and s–d mixing is dependent on the size of the energy separation between the atomic s–p and s-d levels ($\Delta\varepsilon_{sp}$ and $\Delta\varepsilon_{sd}$) and on the size of the dispersion of the s, p, and d bands. The dispersion of the bands is determined by the size of the overlap between the atomic orbitals and by how strongly the valence electrons are bonded to the core of the free atom. The latter is reflected by the energies of the atomic levels ε_s, ε_p, ε_d. As one moves down Group 15, p orbital interactions weakens because p orbitals become more diffuse and higher in energy. At the same time s orbitals become more compact and their energy decreases due to the relativistic effects. Thus, s–p mixing decreases from P to Bi. The ability of s–d mixing is especially pronounced in P. In P d electrons are absent in the core and thus for the 3d valence orbitals there is no repulsive core-orthogonality requirement. The structures A7 and A17 are decisively stabilized by s–p mixing. The more layered A17 structure is realized for P, which displays the largest ability to s–p mixing. The pressure stability of the A7 ground state structure decreases from As to Bi in accordance with decreasing s–p mixing (cf Figure 1). The simple packed structures sc and sh are decisively stabilized by s–d mixing. This mixing is most effective in P. As a consequence, the A7 → sc transition occurs earlier than in heavier As, which violates the tendency for the same transition to occur at lower pressures in the heavier element (i.e. the empirical corresponding-states principle[35]). In general, s–d mixing in P enlarges considerably the range of compression where E^{band} determines structural stability. For the heavier congeners E^{Mad} influences structural stability already in the intermediate pressure region and this leads to the formation of complex structures.

Conclusion

Recently, many surprising and spectacular elemental main-group modifications have been revealed by high-pressure experiments.[1–7] As a matter of fact, these findings challenge our traditional understanding of the relationship between electronic structure and atom arrangement in elemental structures. In most cases the underlying reason for "strange" high-pressure structures is subtle changes of the valence states of the elements under pressure. This influences the one-particle energy (E^{band}) contribution to the total energy. The band energy E^{band} favors the formation of open-packed structures in which the atoms are closer to each other and thus covalent bonding can be realized. This tendency is balanced by the electrostatic energy (E^{Mad}), which stabilizes densely packed high-symmetry structures.

We attempted to rationalize the high-pressure structural sequences of the Group 15 elements P, As, Sb, and Bi on the basis of electronic structure theory. These elements possess the layered structures A7 or A17 under ambient conditions, and the bcc structure as end-member in their high-pressure structural series. The intermediate pressure region displays several peculiarities: P attains the simple sc and sh structure, whereas the heavier congeners prefer a complex host–guest arrangement. We could show that the layered ground state structures are stabilized by s–p mixing, which gradually weakens on going down the group. The simple packed

  0947-6539/03/0907-1477 $ 20.00+.50/0

structures are stabilized by s–d mixing, which is effective especially in P because of the absence of d electrons in the core. The formation of a host–guest structure in the heavier congeners is explained as a consequence of a delicate interplay of the energies E^{band} and E^{Mad} in the intermediate pressure region of As, Sb, and Bi, that is both important parts of the total energy account equally for structural stability.

Computational Methods

Total energy calculations for P and As as a function of volume were performed within ab inito density functional theory using pseudopotentials and a plane wave basis set as implemented in the program VASP.[36] Ultrasoft Vanderbilt-type pseudopotentials[37] were employed and P 3s and 3p, and As 4s and 4p were treated as valence electrons. We considered the elements in the structure types A17 (orthorhombic), A7 (rhombohedral), simple cubic (sc), Bi-III (tetragonal), simple hexagonal (sh), and body centered cubic (bcc). The Bi-III structure corresponds to an incommensurately modulated composite structure. Since conventional electronic structure calculations are based on periodic boundary conditions an incommensurate structure has to be approximated by a supercell. Details of the structural model are given in reference [9]. The atomic position parameters and lattice parameters of the structure types A17, A7, and Bi-III, as well as the axial ratio of the sh structure were relaxed for a set of constant volumes until forces had converged to less than 0.01 eV Å^{-1}. In a second step we fitted the E versus V values of all structures to polynomials whose curvature yielded the pressure. After having obtained the pressure, enthalpies H were calculated according to $H(p) = E(p) + pV(p)$. The exchange and correlation energy was assessed by the generalized gradient approximation (GGA).[38] Convergency of the calculations was carefully checked with respect to the plane wave cutoff and the number of k points used in the summation over the Brillouin zone. Concerning the plane wave cutoff an energy value of 300 eV was chosen for all systems. k points were generated by the Monkhorst–Pack method[39] and sampled on grids of $4 \times 4 \times 4$ (Bi-III type), $13 \times 13 \times 13$ (A17), $15 \times 15 \times 15$ (A7) and $17 \times 17 \times 17$ (sc, sh and bcc types). The integration over the Brillouin zone was performed with a Gaussian smearing of 20 mRy. Total energies were converged to better than 1 meV per atom.

Acknowledgement

This work was supported by the Carl Trygger Foundation.

[1] M. Hanfland, K. Syassen, N. E. Christensen, D. L. Novikov, *Nature* **2000**, *408*, 174.
[2] R. J. Nelmes, M. I. McMahon, J. S. Loveday, S. Rekhi, *Phys. Rev. Lett.* **2002**, *88*, 155503.
[3] M. I. McMahon, R. J. Nelmes, S. Rekhi, *Phys. Rev. Lett.* **2001**, *87*, 255502.
[4] O. Degtyareva, M. I. McMahon, R. J. Nelmes, *40th European High-Pressure Research Group Meeting*, Edinburgh, UK, **2002**.
[5] M. I. McMahon, T. Bovornratanaraks, D. R. Allan, S. A. Belmonte, R. J. Nelmes, *Phys. Rev. B* **2000**, *61*, 3135.
[6] R. J. Nelmes, D. R. Allan, M. I. McMahon, S. A. Belmonte, *Phys. Rev. Lett.* **1999**, *83*, 4081.
[7] a) M. I. McMahon, O. Degtyareva, R. J. Nelmes, *Phys. Rev. Lett.* **2000**, *853*, 4896; b) an incommensurate composite structure has also been reported recently for Rb–IV: M. I. McMahon, S. Rekhi, R. J. Nelmes, *Phys. Rev. Lett.* **2000**, *87*, 055501.
[8] Heine, V. *Nature* **2000**, *403*, 836.
[9] U. Häussermann, K. Söderberg, R. Norrestam, *J. Am. Chem. Soc.* **2002**, *124*, 15359.
[10] J. Donahue, *The Structures of the Elements*, Wiley, New York, **1974**.
[11] J. K. Burdett, S. Lee, *J. Am. Chem. Soc.* **1983**, *105*, 1079.
[12] J. C. Jamieson, *Science* **1963**, *139*, 219.
[13] T. Kikegawa, H. Iwasaki, *Acta Crystallogr. C* **1983**, *39*, 158.
[14] H. J. Beister, K. Strössner, K. Syassen, *Phys. Rev. B* **1990**, *41*, 5535.
[15] D. Schiferl, D. T. Cromer, J. C. Jamieson, *Acta Crystallogr. B* **1981**, *37*, 807.
[16] H. Iwasaki, T. Kikegawa, *High Pressure Res.* **1990**, *6*, 121.
[17] R. M. Brugger, R. B. Bennion, T. G. Worlton, *Phys. Lett.* **1967**, *24A*, 714.
[18] Y. Akahama, M. Kobayashi, H. Kawamura, *Phys. Rev. B* **1999**, *59*, 8520.
[19] R. G. Greene, H. Luo, A. L. Ruoff, *Phys. Rev. B* **1995**, *51*, 597.
[20] Y. Akahama, H. Kawamura, S. Carlson, T. Le Bihan, D. Häusermann, *Phys. Rev. B* **2000**, *61*, 3139.
[21] K. Aoki, S. Fujiwara, M. Kusakabe, *Solid State Comm.* **1983**, *45*, 161.
[22] K. Aoki, S. Fujiwara, M. Kusakabe, *J. Phys. Soc. Jpn.* **1982**, *51*, 3826.
[23] H. Olijnyk, W. B. Holzapfel, *Phys. Lett.* **1984**, *100A*, 191.
[24] H. Olijnyk, S. K. Sikka, W. B. Holzapfel, *Phys. Lett.* **1984**, *103A*, 137; J. Z. Hu, I. L. Spain, *Solid State Comm.* **1984**, *51*, 263.
[25] Y. K. Vohra, K. E. Brister, S. Desgreniers, A. L. Ruoff, *Phys. Rev. Lett.* **1986**, *56*, 1944.
[26] K. J. Chang, M. L. Cohen, *Phys. Rev. B* **1986**, *33*, 6177.
[27] T. Sasaki, K. Shindo, K. Niizeki, A. Morita, *Solid State Commun.* **1987**, *62*, 795.
[28] T. Sasaki, K. Shindo, K. Niizeki, A. Morita, *J. Phys. Soc. Jpn.* **1988**, *57*, 978.
[29] A. Nishikawa, K. Niizeki, K. Shindo, *Phys. Stat. Sol. B* **2001**, *223*, 189.
[30] K. J. Chang, M. L. Cohen, *Phys. Rev. B* **1986**, *33*, 7371.
[31] L. F. Mattheiss, D. R. Hamann, W. Weber, *Phys. Rev. B* **1986**, *34*, 2190.
[32] C. R. S. da Silva, R. M. Wentzcovitch, *Comput. Mater. Sci.* **1997**, *8*, 219.
[33] D. G. Pettifor, *Bonding and Structure of Molecules and Solids*, Clarendon Press, Oxford, **1995**.
[34] D.-K. Seo, R. Hoffmann, *J. Solid State Chem.* **1999**, *147*, 26.
[35] D. A. Young, *Phase Diagrams of the Elements* University of California Press, Berkeley, **1991**.
[36] G. Kresse, J. Hafner, *Phys. Rev. B* **1993**, *47*, 558; G. Kresse, J. Furthmüller, *Phys. Rev. B* **1996**, *54*, 11169.
[37] D. Vanderbilt, *Phys. Rev. B* **1990**, *41*, 7892; G. Kresse, J. Hafner, *J. Phys.: Condens. Matter* **1994**, *6*, 8245.
[38] J. P. Perdew, Y. Wang, *Phys. Rev. B* **1992**, *45*, 13244.
[39] H. J. Monkhurst, J. D. Pack, *Phys. Rev. B* **1976**, *13*, 5188.

Received: October 21, 2002 [F4517]

